# Li/MgO with Spin Sensors as Catalyst for the Oxidative Coupling of Methane

U. Simon[a,*], S. Arndt[b,*], T. Otremba[b], T. Schlingmann[a], O. Görke[a], K.-P. Dinse[c], R. Schomäcker[b], H. Schubert[a,**]

[a] *Technische Universität Berlin, Department of Material Science, Englische Straße 20, 10587 Berlin, Germany*
[b] *Technische Universität Berlin, Department of Chemistry, Straße des 17. Juni 124, 10623 Berlin, Germany*
[c] *Freie Universität Berlin, Arnimallee 14, 14195 Berlin, Germany*

**Abstract**

Co-doping of Li/MgO, a well-known catalyst for the oxidative coupling of methane, was investigated. It is demonstrated that $Gd^{3+}$ and $Fe^{3+}$ can be used as spin sensors in these solids to investigate the structure via EPR spectroscopy. These aliovalent ions occupy $Mg^{2+}$ sites in the lattice; the expected coupling with charge-compensating neighboring $Li^{+}$ was detected. A strong increase of the activity was observed. However, all samples suffered from deactivation. The solubility of $Gd^{3+}$ in MgO turned out to be inhibited. No such restriction was observed for $Fe^{3+}$.

*Keywords:* Oxidative Coupling of Methane, Li/MgO, Transition Metal Oxides, Rare Earth Oxide, Cation Substitution, Spin Sensor, EPR

## 1. Introduction

The oxidative coupling of methane (OCM) (Equation 1) is an attractive direct route for the conversion of methane into value added compounds. Li/MgO was considered to be a potential candidate for a practical application, despite the doubts on the stability.

$$CH_4 + O_2 \rightarrow C_2H_6 \text{ or } C_2H_4 + H_2O \qquad (1)$$

A very detailed investigation has shown, that it suffers from an intrinsic instability [1–3], prohibiting any practical application. Furthermore, Li evaporates from the catalyst and only a content of approximately 0.01 - 0.03 wt% Li in MgO is stable [1, 2, 4].

To improve the catalytic performance of Li/MgO, it was doped with numerous additional metal oxides [5–24]. In many cases an improved stability and/or higher selectivity was found, however, deactivation of these catalysts was often retarded, but still observed.

Moreover, doping did not contribute to an understanding of the catalytic system. In an excellent review article, Gellings and Bouwmeester commented that unfortunately many of the publications, dealing with co-doped Li/MgO, have not interpreted the results in terms of the charge compensating defects and the influence of the dopants thereon [25].

The present study shows how the co-dopants Fe and Gd can be used as spin sensors for the EPR spectroscopy to investigate the structure of such materials. Fe and Gd have been chosen as co-dopants, not because they could result in a better catalytic performance then compared to catalysts reported in the literature, but because because these high spin ions can serve as sensitive probes for the local structure. However, the anticipated stabilization of the Li-content by these charge compensating ions ($Gd^{3+}$, $Fe^{3+}$) might lead to an improved stability of the catalytic performance.

## 2. Experimental Part

### 2.1. Preparation

In a catalyst the content of the different metal oxides is calculated in atom percent (at%) based on the total cation content, shown in Equation 2.

$$\text{Cation A [at\%]} = \frac{\text{Cation A [mol]}}{\sum \text{all Cations [mol]}} \times 100\% \qquad (2)$$

Aqueous solutions of $Mg(NO_3)_2$ were prepared by dissolving $Mg(NO_3)_2 \times 6H_2O$ (p.A., Merck) in distilled $H_2O$. The solution of $Fe(NO_3)_3 \times 9H_2O$ (p.A., Riedel de Haen) and $Gd(NO_3)_3 \times 6H_2O$ (99,9 %, Sigma Aldrich) was prepared the same way. The nitrate solutions were

*These authors contributed equally; the order was determined by Paper, Scissors, Stone.
**Corresponding Author. Fax: 0049-30-314-28534, Tel: 0049-30-314-24833
*Email address:* schubert@ms.tu-berlin.de (H. Schubert)

concurrently added drop wise to stirred ammonia solution while keeping the pH value above 11. The gelatinous precipitates were rinsed with distilled $H_2O$ and mixed with aqueous LiOH solution ($LiOH \times H_2O$ p.A., Riedel de Haen) with appropriate Li concentrations in a tubular mixer. The prepared combination of oxides were:

1. MgO
2. Gd/MgO
3. Gd-Li/MgO
4. Fe-Li/MgO

Finally, the solution was quick-frozen using liquid $N_2$. Afterwards, it was freeze-dried over at least 72 h using a freeze-dryer (Gamma 2-20 (Christ)). Finally, the samples were calcined at 900 $°C$ for 1 h in MgO crucibles. A scheme of the preparation procedure is shown in Figure 1.

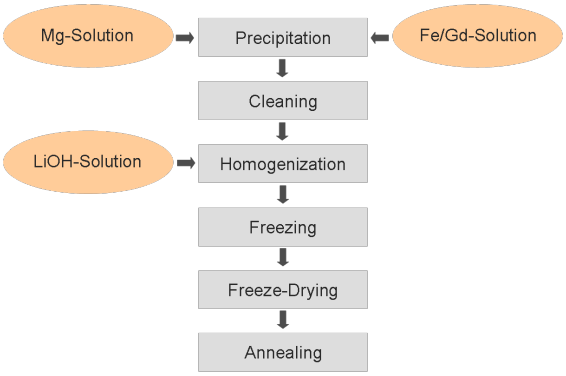


Figure 1: Delineation of the applied preparation procedure.

Some samples were too fluffy after calcination; therefore, they were pressed at 100 bar for 10 minutes and subsequently crushed. All samples were sieved and only the fraction $\leq 200\,\mu m$ was used for testing to exclude internal mass transfer effects.

### 2.2. Characterization

The Li-content of the different samples was quantified via atomic absorption spectroscopy, using a AAS NovAA 400 G device from Analytik Jena via flame.

The Fe and Gd-content was determined via inductively coupled plasma atomic emission spectroscopy, using a Horiba Scientific ICP Model Ultima 2.

The specific surface area was determined by a Micromeritics Gemini III 2375 Surface Area Analyzer, using $N_2$ adsorption at -196 $°C$. Before measuring, the samples were degassed at 300 $°C$ and 0.15 mbar at least for 30 minutes. The surface areas were calculated by the method of Brunauer, Emmett and Teller.

Powder X-Ray diffractograms were obtained (CuK$\alpha$1 radiation, with a wavelength 0.154 nm) using a Bruker AXS D8 ADVANCE X-ray diffractometer.

EPR experiments were performed with a BRUKER E680 spectrometer. The spectrometer was operated in conventional continuous wave (cw) as well as in pulsed mode. Data were taken from "as prepared" compounds.

### 2.3. Catalysis

A 6-fold parallel reactor (Integrated Lab Solutions Berlin and Premex Reactor AG) was used for the determination of the catalytic activity, with packed-bed, linear, tubular reactors made of quartz glass. For each catalytic run, 50 mg catalyst were diluted with approximately 1.5 ml quartz sand (Merck). Below and above the catalyst bed, a small amount of pure quartz sand was put to ensure proper heat transfer. The applied reaction conditions were: 750 $°C$ reactor temperature, 60 ml/min gas flow and a feed gas composition of $CH_4$:$O_2$:$N_2$ = 4:1:4. The analysis was performed with a gas chromatograph Agilent 7890 A. The conversion and selectivity is calculated with a mass balance based on the inlet and outlet concentration of reactants and products, see Equations 3 and 4, taking into account the different numbers of C-atoms in the different molecules. The carbon balance was always well above 95 %. The formation of CO was not observed in any of the experiments, $CO_2$ was the only observed total oxidation product and and no visible formation of deposited carbon was found.

$$X = \frac{\sum(\text{Reaction Products})}{\sum(\text{Reaction Products}) + \text{unconverted Reactant}} \tag{3}$$

$$S_A = \frac{\text{Product A}}{\sum(\text{Reaction Products})} \tag{4}$$

## 3. Results and Discussion

In Table 1 an overview over the target and the actual loading of Li and the Gd or Fe-content, the BET surface area and the present phases, detected via XRD is given. The intended and the loading of Li, Fe and Gd of the prepared catalysts agree very well. The ratio TM/Li is in both cases near 1 and the BET surface area does not vary too strongly.

XRD patterns of the Gd-Li/MgO sample indicate the formation of $Gd_2O_3$ besides the main phase MgO, shown in Figure 2. Thus, a low solubility of $Gd^{3+}$ in

Table 1: Li, Gd and Fe-content of the different catalysts, the ratio dopant to Li, the specific surface area, determined before reaction, the sample color and the detected phases.

| | Target-Content | | Measured-Content | | Atom Ratio | BET | Color | XRD Phases |
|---|---|---|---|---|---|---|---|---|
| Catalyst | Li [at%] | Dop. [at%] | Li [at%] | Dop. [at%] | [Dop./Li] | [$m^2/g$] | | |
| MgO | - | - | - | - | - | 34.4 | white | MgO |
| Gd/MgO | - | 0.7 | - | 0.7 | - | 37.0 | white | MgO, $Gd_2O_3$ |
| Fe-Li/MgO | 0.5 | 0.5 | 0.5 | 0.5 | 1.0 | 29.4 | light yellow | MgO |
| Gd-Li/MgO | 0.7 | 0.7 | 0.7 | 0.8 | 1.1 | 16.7 | white | MgO, $Gd_2O_3$ |

MgO can be assumed, which could be caused by the larger ionic radius of $Gd^{3+}$ of 94 pm (coordination number 6) compared to the radius of $Mg^{2+}$ of 72 pm (coordination number 6). No such restrictions were observed for $Fe^{3+}$ (ionic radius: 55 pm for coordination number 6). The Fe-Li/MgO sample showed solely the XRD peaks of the MgO phase indicating an entire incorporation of the Li and Fe ions in MgO. The peak positions of the MgO pattern were marginally affected. An overview of the detected phases is shown in Table 1.

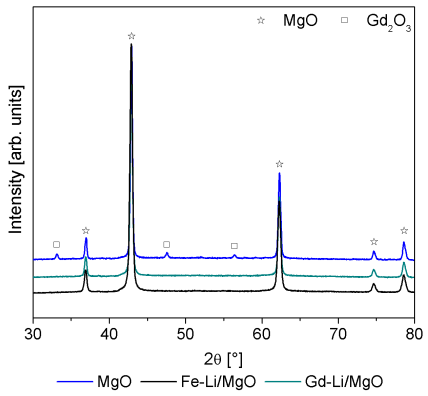


Figure 2: XRD patterns of MgO, Fe-Li/MgO and Gd-Li/MgO (bottom to top).

EPR spectra of Gd-Li/MgO samples exhibit the characteristic powder pattern of $Gd^{3+}$ in its S = 7/2 spin state. Replacing $Mg^{2+}$ substitutionally, the local site symmetry significantly restricts the number of spin Hamilton parameters as was described by Abraham *et al.* for a single crystal of MgO [27]. For co-doping, local $Gd^{3+}$ - $Li^{+}$ clusters are anticipated. Such an arrangement would break the local site symmetry, introducing for instance otherwise forbidden second rank tensor elements. For the Gd-Li/MgO sample, a small but significant deviation from the single crystal parameter set [27] is found, as expected being caused by co-doping with Li. Comparing with Gd/MgO powder samples, an almost identical EPR pattern is observed (see Figure 3). Apparently, the preparation and sintering process used induces

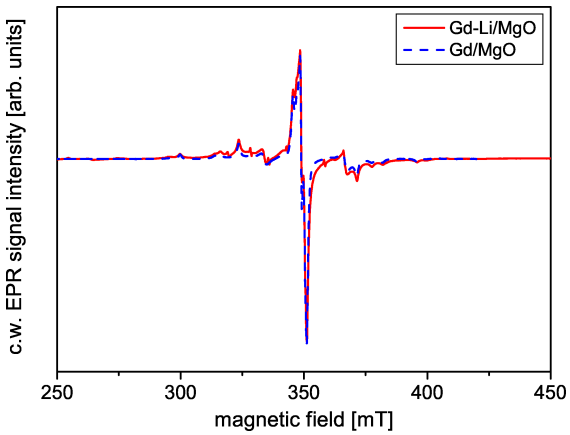


Figure 3: EPR spectra of Gd/MgO (blue trace) and Gd-Li/MgO (red trace) taken at 80 K. The narrow spikes can be attributed to trace amounts of $Mn^{2+}$.

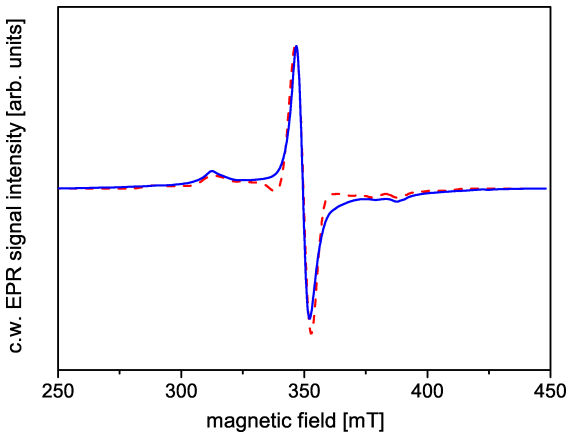


Figure 4: EPR spectrum of Fe-Li/MgO taken at 80 K. The dotted line is a least squares fit resulting in $B_{40}$ = 5 MHz and $B_{44}$ = 30 MHz, quite close to the values of 5.16 MHz and 25.6 MHz, determined by Boldu *et al.* from single crystals data [26].

distortions from perfect cubic symmetry, which in turn also lead to the appearance of the observed additional spin Hamilton parameters. Using pulsed EPR instead of conventional cw detection, a true EPR absorption spectrum can be detected instead of a field derivative pattern. Using this detection method, additional broad signals covering a much larger field range from 220 to 480 mT could be recorded exclusively for the co-doped sample, indicative of a significant distortion of the local symmetry. We ascribe this pattern as resulting from the formation of next neighbor correlated pairs. A detailed analysis will be presented in a forthcoming publication.

Cw EPR signals observed for the Fe-Li/MgO powder samples can be fitted by using spin Hamilton parameters very similar to the parameter set reported by Boldu *et al.* for Fe-doped single crystals of MgO [26], as shown in Figure 4. This indicates that the topology of the Fe site is not significantly disturbed by adjunct Li ions. Because of very fast spin relaxation, no pulsed EPR spectra could be detected. For this reason no effect of co-doping could be detected by EPR for this compound.

The $CH_4$ conversion, the selectivity for $C_2$ and $CO_2$ (CO formation was not observed) for all 3 materials is shown in Figure 5. The catalytic performance of pure MgO is low, however, it does not deactivate significantly.

Co-doping with charge compensating Fe leads to a significantly increased $CH_4$ conversion, however, total oxidation prevails. Using Gd instead for charge compensation, an initial activity comparable with Fe-Li/MgO at a significantly higher $C_2$ selectivity, however the XRD results indicate a formation of $Gd_2O_3$ beside Gd-MgO solid solution. This could be responsible for the higher activity, as $Gd_2O_3$ exhibits a considerable OCM activity [28]. However, this catalysts also suffers from deactivation. A steady state has not been reached within 16 h.

## 4. Summary and Conclusion

Co-doping of Li/MgO catalysts with charge compensating ions was performed with a constant atomic ratio of Li to dopant of 1:1. These aliovalent ions turned out to occupy $Mg^{2+}$ sites in the lattice. The solubility of $Gd^{3+}$ in MgO turned out to be limited. No such restrictions were observed for $Fe^{3+}$. The anticipated Li-stabilization by co-doping Li/MgO with $Fe^{3+}$ and $Gd^{3+}$ apparently seems to take place. An indication of the expected coupling with charge compensating neighboring $Li^{+}$ was detected via EPR for the Gd-Li/MgO sample. Therefore, the application potential of dopants as EPR spin sensors for solids has been demonstrated.

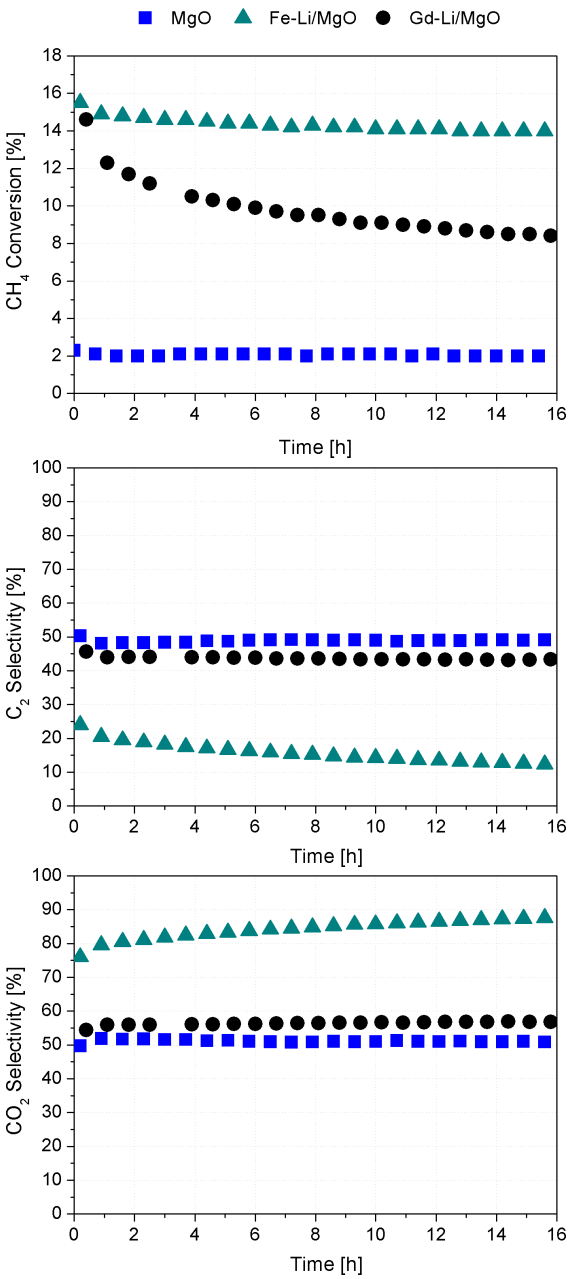


Figure 5: The $CH_4$ conversion (top) and the $C_2$ selectivity (middle) and the selectivity for $CO_2$ (CO formation was not observed) for MgO, Fe-Li/MgO and Gd-Li/MgO.

The co-doping results in active catalytic materials, however, deactivation is not suppressed. Doping with Fe leads to a significantly increased $CH_4$ conversion, however, total oxidation is dominating. Gd-Li/MgO showed an improved performance with respect to conversion and selectivity, however, the activity might be due to the formation of $Gd_2O_3$ on the MgO, as detected via XRD.

## Acknowledgment

This work is part of the Cluster of Excellence "Unifying Concepts in Catalysis" coordinated by the Technische Universität Berlin. Financial support by the Deutsche Forschungsgemeinschaft (DFG) within the framework of the German Initiative for Excellence is gratefully acknowledged. We thank Prof. Thomas for the permission to use his XRD diffractometer.

## References

[1] S. Arndt. *Stability of Lithium doped Magnesium Oxide and Zinc Oxide Catalysts for the Conversion of Natural Gas*. PhD thesis, Technical University Berlin, 2010.

[2] S. Arndt, U. Simon, S. Heitz, A. Berthold, B. Beck, O. Görke, J.D. Epping, T. Otremba, Y. Aksu, E. Irran, G. Laugel, M. Driess, H. Schubert, and R. Schomäcker. Li-doped MgO From Different Preparative Routes For The Oxidative Coupling Of Methane. *submitted to Top. Catal.*

[3] S. Arndt, G. Laugel, S. Levchenko, R. Horn, M. Baerns, M. Scheffler, R. Schlögl, and R. Schomäcker. Li/MgO - The Drosophila Catalyst for Methane Oxidative Coupling. A Critical Assessment. *submitted to Catal. Rev. Sci. Eng.*

[4] A.G. Anderson and T. Norby. Liquid Phases in Li:Mgo as studied by thermoanalytical Methods, Electron Microscopy, and Electrical Conductivity Measurements. *Catal. Today*, 6:575–586, 1990.

[5] F.P. Larkins and M.R. Nordin. The Effects of Transition Metal Oxides on the Methane Oxidative Coupling Activity of doped MgO Catalysts I. Zinc and Manganese. *J. Catal.*, 130:147–160, 1991.

[6] S.J. Korf, J.A. Roos, L.J. Veltman, J.G. van Ommen, and J.R.H. Ross. Effect of Additives on Lithium Doped Magnesium Oxide Catalysts used in the Oxidative Coupling of Methane. *Appl. Catal*, 56:119–135, 1989.

[7] R. Mariscal, J. Soria, M.A. Pena, and J.L.G. Fierro. Features of Li-Mn-MgO Catalysts and Their Relevance in the Oxidative Coupling of Methane. *J. Catal.*, 147:535–543, 1994.

[8] V.R. Choudhary, A.M. Rajput, D.B. Akolekar, and V.A. Seleznev. Oxidative Conversion of Methane to $C_2$-Hydrocarbons over Lithium, Manganese, Cadmium and Zinc promoted MgO Catalysts I. Catalyst Performance in Presence of Free Oxygen. *Appl. Catal*, 62:171–187, 1990.

[9] V.R. Choudhary, S.D. Sansare, A.M. Rajput, and D.B. Akolekar. Oxidative Conversion of Methane to $C_2$-Hydrocarbons over Li, Mn, Cd and Zn promoted MgO Catalysts II: Performance of fresh and reoxidised catalysts in the absence of free oxygen. *Appl. Catal*, 69:187–200, 1991.

[10] T. Kanno and M. Kobayashi. The difference in the modification effects of Li on two MgO samples of higher and lower Mn contents. *J. Mater. Sci. Lett.*, 16:126–127, 1997.

[11] J.J. Zhang, X.G. Yang, Y.L. Bi, and K.J. Zhen. Role of Li Ion in Li-Mn-MgO Catalyst for Oxidative Coupling of Methane. *Catal. Today*, 13:555–558, 1992.

[12] F.P. Larkins and M.R. Nordin. Physico-Chemical and Catalytic Properties of Doped MgO Catalysts. *Stud. Surf. Sci. Catal.*, 81:249–251, 1994.

[13] D.J. McNamara, S.J. Korf, K. Seshan, J.G. van Ommen, and J.R.H. Ross. The Effect of $Nb_2O_5$ and $ZrO_2$ Additions on the Behavior of Li/MgO and Li/Na/MgO Catalysts for the Oxidative Coupling of Methane. *Can. J. Chem. Eng.*, 69:883–890, 1991.

[14] G.C. Hoogendam, K. Seshan, J.G. van Ommen, and J.R.H. Ross. Oxidative coupling of methane over doped Li/MgO catalysts. *Catal. Today*, 21:333–340, 1994.

[15] S.J. Korf, J.A. Ross, J.A. Vreeman, J.W.H.C. Derksen, J.G. van Ommen, and J.R.H. Ross. A Study of the Kinetics of the Oxidative Coupling of Methane over a Li/Sn/MgO catalyst. *Catal. Today*, 6:417–426, 1990.

[16] A.N.J. van Keulen, G.C. Hoogendam, K. Seshan, J.G. van Ommen, and J.R.H. Ross. The Role of Tin in Li/Sn/MgO Catalysts for the Oxidative Coupling of Methane. *J. Chem. Soc., Chem. Commun.*, 18:1546–1547, 1992.

[17] R.H. Nibbelke, J. Scheerová, M.H.J.M. de Croon, and G.B. Marin. The Oxidative Coupling of Methane over MgO-Based Catalysts: A Steady-State Isotope Transient Kinetic Analysis. *J. Catal.*, 106:106–119, 1995.

[18] E.P.J. Mallens, J.H.B.J. Hoebink, and G.B. Marin. An Investigation of the Oxygen Pathways in the Oxidative Coupling of Methane over MgO-Based Catalysts. *J. Catal.*, 160:222–234, 1996.

[19] K. Nagaoka, T. Karasuda, and K.I. Aika. The Effect of $SnO_2$ Addition to Li/MgO Catalysts for the Oxidative Coupling of Methane. *J. Catal.*, 181:160–164, 1999.

[20] Y.L. Bi, K.J. Zheng, Y.T. Jiang, C.W. Teng, and X.G. Yang. Catalytic Oxidative Coupling of Methane over Alkali, Alkaline Earth and Rare Earth Metal Oxides. *Appl. Catal*, 39:185–190, 1988.

[21] S. Bartsch, J. Falkowski, and H. Hoffmann. Catalyst Development for Oxidative Methane Coupling. *Catal. Today*, 4:421–431, 1989.

[22] S. Bartsch and H. Hoffmann. Investigations on a Ce/Li/MgO-Catalyst for the Oxidative Coupling of Methane. *Catal. Today*, 6:527–534, 1990.

[23] A. Santos, C. Finol, J. Coronas, M. Menéndez, and J. Santamaría. Reactor Engineering Studies of Methane Oxidative Coupling on a Li/MgO Catalyst. *Stud. Surf. Sci. Catal.*, 81:171–176, 1994.

[24] A. Santos, M. Menéndez, and J. Santamaría. Oxidative coupling of methane over Li/Sn/MgO catalysts. Use of a fluidized bed reactor at low gas velocities. *Stud. Surf. Sci. Catal.*, 107:373–378, 1997.

[25] P.J. Gellings and H.J.M. Bouwmeester. Solid state aspects of oxidation catalysis. *Catal. Today*, 58:1–53, 2000.

[26] J.L. Boldú, E. Munoz, Y. Chen, and M.M. Abraham. EPR power pattern analysis for cubic sites of $Fe^{3+}$ in MgO. *Journal of Chemical Physics*, 80:574–575, 1984.

[27] M.M. Abraham, L.A. Boatner, Y. Chen, J.L. Kolopus, and R.W. Reynolds. Cubic-Site EPR Spectra of $Eu^{2+}$ and $Gd^{3+}$ in MgO Single Crystals. *Physical Review B*, 4:2853–2857, 1971.

[28] O. Forlani and S. Rossini. Rare earths as catalysts for the oxidative coupling of methane to ethylene. *Mater. Chem. Phys.*, 31:155–158, 1992.